An Adaptive Iterative Symbol Clipping Scheme For OFDM-Based Visible Light Communication

Kejun Jia (kjjia@lut.cn)
Lanzhou University of Technology https://orcid.org/0000-0002-5213-0283
Cuicui Qin
Lanzhou University of Technology
Boran Yang
Southwest Jiaotong University
Minghua Cao
Lanzhou University of Technology
Suoping Li
Lanzhou University of Technology

Research Article

Keywords: Visible light communication, Optical OFDM, LED nonlinear, Clipping distortion

Posted Date: October 22nd, 2021

DOI: https://doi.org/10.21203/rs.3.rs-995314/v1

An Adaptive Iterative Symbol Clipping Scheme for OFDM-based Visible Light Communication

Kejun Jia[1*], Cuicui Qin[1†], Boran Yang[3†], Minghua Cao[1†] and Suoping Li[2†]

[1*]School of Computer and Communication, Lanzhou University of Technology, Lanzhou, Gansu, 730050, China.
[2]School of science, Lanzhou University of Technology, Lanzhou, Gansu, 730050, China.
[3]School of Information Science and Technology, Southwest Jiaotong University, Chengdu, Sichuan, 610031, China.

*Corresponding author(s). E-mail(s): kjjia@lut.cn;
Contributing authors: 18143752125@163.com;
†These authors contributed equally to this work.

Abstract

In this paper, an adaptive iterative symbol clipping scheme for OFDM-based visible light communication systems is proposed. This scheme can avoid the disadvantages of the conventional iterative signal clipping (ISC) scheme that produces all-zero symbols due to the fixed iterative clipping times, and also avoids the information transmission rate degradation due to an adaptive symbol decomposition with serial transmission (ASDST) scheme using serial transmission. In the proposal, optical orthogonal frequency division multiplexing (O-OFDM) symbols are decomposed into multiple O-OFDM symbols that are in the linear range of the LEDs after adaptive iterative clipping according to the signal amplitude and clipping threshold, thereafter simultaneously transmitted through multiple LEDs. When the number of LEDs is large enough, clipping distortion can be significantly reduced or even completely eliminated. In addition, the all-zero symbols existing in the ISC scheme can be completely eliminated. Experimental results show that the proposed scheme can not only improve the BER performance and the optical power efficiency, but also reduce the clipping times compared with

the traditional ISC scheme. Besides,our proposed scheme could achieve higher information transmission rate compared with the ASDST scheme.

Keywords: Visible light communication, Optical OFDM, LED nonlinear, Clipping distortion

1 Introduction

With the rapid development of Internet technology, the demand for mobile data is exploding, which has caused the spectrum deficit in current radio frequency (RF) technologies. Visible light communication (VLC) not only can solve the problem of spectrum scarcity, but also has the potential to surpass the high data rate requirements of 5G systems. Therefore it is expected to be a key technology for the next generation mobile communication system.

Orthogonal frequency division multiplexing (OFDM) technology has gained wide application in the field of RF because of its high transmission speed and strong resistance to inter-symbol interference (ISI). Meanwhile, it is also greatly concerned in the scenario of VLC. Different from RF communication, VLC transmits the wireless data through Intensity Modulation and Direct Detection (IM/DD)[1], which the OFDM signal driving the light emitting diodes (LED) must be real and unipolar. Therefore, it is necessary to modify the OFDM signal in RF communication to meet the requirements of IM/DD systems[2]. Two optical OFDM (O-OFDM) transmission schemes are considered in this paper, i.e., asymmetrically clipped O-OFDM (ACO-OFDM)[3] and direct current biased O-OFDM (DCO-OFDM)[4]. O-OFDM inherits the advantages of traditional OFDM, but also inevitably inherits the inherent disadvantages of OFDM, such as the high peak-to-average power ratio (PAPR). Because of this drawback, the O-OFDM signal can easily exceed the linear operating range of the optoelectronic device, which causing serious nonlinear effects, and degrading the bit error rate (BER) and the error vector magnitude (EVM) performance[5]. LEDs are one of the main sources of nonlinearity in VLC, so a proper understanding and treatment of LED nonlinearity is essential for the implementation of O-OFDM based visible light communication.

Solutions to the problem of non-linear distortion in VLC can generally be divided into two categories. The first category is to linearize the nonlinear transmission characteristics of LEDs by methods such as pre-distortion or post-distortion. The pre-distortion method in[6, 7] compensates the nonlinearity of LEDs by designing physical analogue circuits. However, the pre-distortion method is difficult to be widely used because the transmitter requires additional feedback physical circuits. In[8], the proposed post-distortion technique compensates the LED nonlinearity by means of a Volterra receiver. An adaptive digital post-distortion technique for DCO-OFDM systems was proposed in[9], which can be implemented using a microprocessor. However, the post-distortion technique has disadvantages such as computational complexity and

processing delay. The second category is to reduce the PAPR[10]. Within the dynamic range of the LED, signal after PAPR reduction is less susceptible to non-linearity as compared to the original input signal. Among PAPR reduction algorithms proposed for O-OFDM, distortion-based methods are particularly favored for practical scenarios because the modification of the receiver is avoided[11]. In distortion-based methods, clipping is the simplest method to reduce the PAPR of O-OFDM signals. However, when the signal-to-noise ratio (SNR) is small, there will be clipping distortion on all the sub-carriers in the frequency domain by direct clipping and this distortion will dominate the noise source. Therefore, it is crucial to study how to reduce the clipping noise to improve the system performance[12].

In [13, 14], an iterative signal clipping (ISC) sc3heme is proposed to reduce the clipping distortion. The O-OFDM symbols can be decomposed into multiple O-OFDM symbols within the dynamic range of the LED by iterative clipping. Then, the resulting O-OFDM symbols are simultaneously transmitted through multiple LEDs. When the number of LEDs is large enough, the clipping noise can be significantly eliminated. However, because the clipping times is fixed in this scheme, when the amplitude of O-OFDM symbols is lower, all-zero symbols will appear, which then causes the degradation of BER performance and optical power efficiency.

In [15], an adaptive symbol decomposition with serial transmission (ASDST) scheme is proposed to reduce clipping distortion. According to the signal amplitude, the O-OFDM symbols can be decomposed into multiple O-OFDM symbols within the dynamic range of the LEDs by adaptive iterative clipping. Then, the decomposed multiple O-OFDM symbols are fed into single LED by using serial framing. In comparison with the ISC scheme, the iterative clipping times in this scheme are determined adaptively by the signal amplitude, and can avoid the appearance of all-zero symbols and improve the BER performance and optical power efficiency. This improvement comes at the expense of the information transmission rate.

In this paper, an adaptive iterative symbol clipping (AISC) scheme is proposed to reduce clipping distortion. According to the signal amplitude, the O-OFDM symbols can be decomposed into multiple O-OFDM symbols within the dynamic range of the LEDs by adaptive iterative clipping. Then the decomposed multiple O-OFDM symbols are simultaneously transmitted through multiple LEDs. Through adaptive iterative signal clipping to eliminate all-zero symbols, the decomposed symbols are simultaneously transmitted through multiple LEDs, which improves the BER performance and optical power efficiency, and ensures the information transmission rate.

The remainder of this paper is organized as follows. In Section 2, we describe the principle of O-OFDM system applying AISC scheme. In Section 3, we give the experimental results and performance analysis. Finally, the paper is summarized in Section 4.

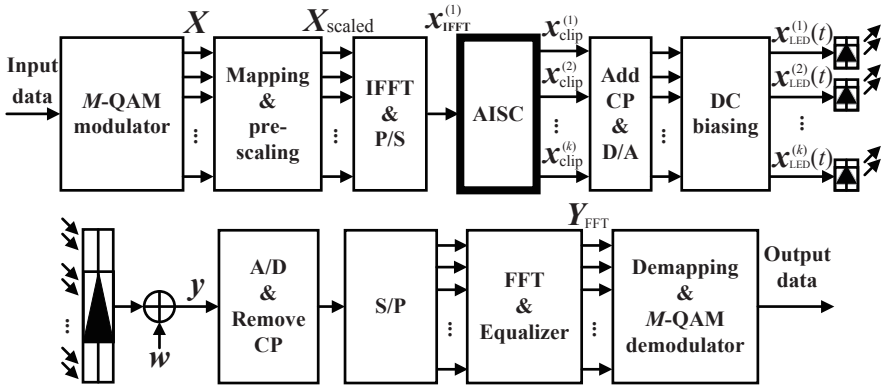

Fig. 1 Block diagram of the O-OFDM system model applying the AISC scheme

2 System Model

2.1 Transmitter

The O-OFDM system model applying the AISC scheme considered in this study is illustrated in Fig.1. Firstly, the input bit stream is modulated according to the adopted M-QAM (Multi-level Quadrature Amplitude Modulation) modulation to produce complex frequency domain symbol $X(l)$ (in ACO-OFDM $l = 0, 1, \cdots, N/4-1$ and in DCO-OFDM $l = 0, 1, \cdots, N/2-1$), where N is the number of subcarriers. In order to ensure the time domain signal is real-valued in O-OFDM, both schemes imposed Hermitian symmetry on the OFDM frame so that the second half of the mapped symbol is a complex conjugate of the first half. The frame structure of the mapped symbols for ACO-OFDM and DCO-OFDM are respectively as follows:

$$\boldsymbol{X}_{\mathsf{mapping}}^{(\mathsf{ACO})} = [0\ X(0)\ 0\ X(1) \cdots X(N/4-1)\ 0\ X^*(N/4-1)\ 0 \cdots X^*(0)]^{\mathrm{T}}, \quad (1)$$

$$\boldsymbol{X}_{\mathsf{mapping}}^{(\mathsf{DCO})} = [0\, X(1)\, X(2) \cdots X(N/2-1)\, 0\, X^*(N/2-1) \cdots X^*(2)\, X^*(1)]^{\mathrm{T}}, \quad (2)$$

where $(\cdot)^*$ denotes the conjugate operation and $(\cdot)^{\mathrm{T}}$ denotes the matrix transpose.

To study the relationship between the O-OFDM symbol variance σ_0^2 and the clipping times, the pre-scale factor is introduced. The mapped symbols are pre-scaled by the pre-scale factor. The pre-scaled symbol can be expressed as follows:

$$\boldsymbol{X}_{\mathsf{scaled}} = \alpha \boldsymbol{X}_{\mathsf{mapping}}, \quad (3)$$

where α is the pre-scale factor and it is derived as follows[15]:

$$\alpha = \sigma_0 \sqrt{\frac{N-1}{\sum_{n=0}^{N-1} |\ \boldsymbol{X}_{\mathsf{mapping}}(n)\ |^2}}. \quad (4)$$

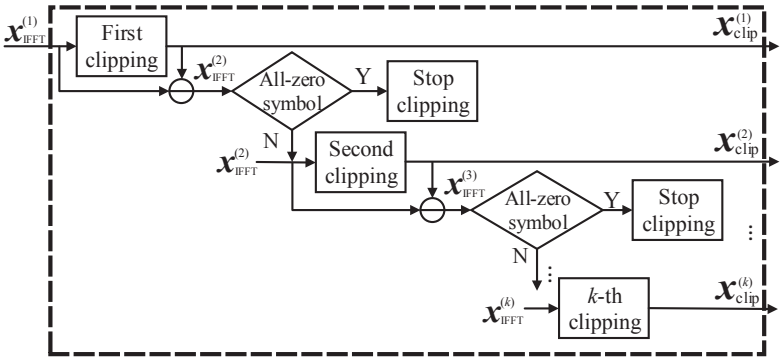

Fig. 2 Block diagram of the detailed implementation processes of the AISC scheme

Note that the variance of α can be calculated as $\mathrm{E}[\alpha^2] = \sigma_0^2/\zeta$, where ζ is the bandwidth efficiency factor and $\mathrm{E}(\cdot)$ is the expectation operator. According to the mapped symbol structure, $\zeta_{\mathsf{ACO}} = 1/2$ for ACO-OFDM system and $\zeta_{\mathsf{DCO}} = (N-2)/N$ for DCO-OFDM system. Hence, the average electrical symbol power of data subcarriers can be denoted as $P_{\mathsf{s,elec}} = \sigma_0^2/\zeta$.

Next, the pre-scaled symbols are subjected to the inverse fast Fourier transform (IFFT) to generate bipolar real-valued time domain signals $\boldsymbol{x}_{\mathsf{IFFT}}$. The output symbol of the IFFT is:

$$\boldsymbol{x}_{\mathsf{IFFT}} = \boldsymbol{F}^{\mathsf{H}} \boldsymbol{X}_{\mathsf{scaled}}, \tag{5}$$

where $(\cdot)^{\mathsf{H}}$ denotes the complex conjugate transpose, $\boldsymbol{F}$ denotes the unitary discrete Fourier transform matrix[15]. According to the central limit theorem (CLT)[16], for larger IFFT sizes, i.e., the total number of subcarriers is greater than 64, the time domain signal $\boldsymbol{x}_{\mathsf{IFFT}}$ approaches a Gaussian distribution with zero mean and variance of $\sigma_0^2 = \mathrm{E}[\boldsymbol{x}_{\mathsf{IFFT}}^2]$.

In order to fit the signal within the dynamic range of the LED, the AISC scheme is proposed. The O-OFDM symbols are decomposed into multiple O-OFDM symbols of smaller amplitude by iterative symbol clipping. The iterative symbol clipping times are determined adaptively according to the amplitude of each O-OFDM symbols, where the permissible maximum iterative clipping times are determined by the number of LEDs and the total number of LEDs is K. The detailed implementation processes of the AISC scheme for the symbol $\boldsymbol{x}_{\mathsf{IFFT}}^{(1)}$ are shown in Fig. 2, where the symbol $\boldsymbol{x}_{\mathsf{IFFT}}^{(1)}$ is obtained after the parallel-to-serial (P/S) conversion of $\boldsymbol{x}_{\mathsf{IFFT}}$. The implementation processes of the AISC scheme can be divided into three steps as follows:

Step 1: The symbol $\boldsymbol{x}_{\mathsf{IFFT}}^{(k)}$ is clipped to get the symbol $\boldsymbol{x}_{\mathsf{clip}}^{(k)}$, where k is the actual iterative symbol clipping times at this time and $k = 1, 2, \cdots, K$.

Step 2: The symbol $\boldsymbol{x}_{\mathsf{clip}}^{(k)}$ is subtracted from the symbol $\boldsymbol{x}_{\mathsf{IFFT}}^{(k)}$ to obtain the symbol $\boldsymbol{x}_{\mathsf{IFFT}}^{(k+1)}$.

Step 3: Determine whether the symbol $\boldsymbol{x}_{\mathsf{IFFT}}^{(k+1)}$ is an all-zero symbol, and stop clipping if the symbol $\boldsymbol{x}_{\mathsf{IFFT}}^{(k+1)}$ is an all-zero symbol (i.e., the implementation processes of the AISC scheme is finished), otherwise set $k = k + 1$ (i.e., $\boldsymbol{x}_{\mathsf{IFFT}}^{(k)} = \boldsymbol{x}_{\mathsf{IFFT}}^{(k+1)}$) and continue to execute step 1 to step 3 until $k = K$.

When the above process is finished, k symbols with the smaller amplitude will be obtained, which are $\boldsymbol{x}_{\mathsf{clip}}^{(1)}, \boldsymbol{x}_{\mathsf{clip}}^{(2)}, \cdots, \boldsymbol{x}_{\mathsf{clip}}^{(k)}$ respectively, in which the k-th symbol can be expressed as:

$$\boldsymbol{x}_{\mathsf{clip}}^{(k)} = \begin{cases} \varepsilon_{\mathsf{top}} & \boldsymbol{x}_{\mathsf{IFFT}}^{(k)} \geq \varepsilon_{\mathsf{top}} \\ \boldsymbol{x}_{\mathsf{IFFT}}^{(k)} & \varepsilon_{\mathsf{bottom}} \leq \boldsymbol{x}_{\mathsf{IFFT}}^{(k)} \leq \varepsilon_{\mathsf{top}} \\ \varepsilon_{\mathsf{bottom}} & \boldsymbol{x}_{\mathsf{IFFT}}^{(k)} \leq \varepsilon_{\mathsf{bottom}}, \end{cases} \tag{6}$$

where, $\varepsilon_{\mathsf{top}}$ and $\varepsilon_{\mathsf{bottom}}$ are the top and bottom clipping levels, respectively. Suppose the dynamic range of LEDs is $V_{\mathsf{min}} \sim V_{\mathsf{max}}$. In addition, the DC bias, B_{DC}, is required to generate a non-negative signal that can drive the LEDs. In ACO-OFDM $\varepsilon_{\mathsf{top}}^{(\mathsf{ACO})} = V_{\mathsf{max}} - B_{\mathsf{DC}}$ and $\varepsilon_{\mathsf{bottom}}^{(\mathsf{ACO})} = \mathsf{max}(V_{\mathsf{min}} - B_{\mathsf{DC}}, 0)$, where $\mathsf{max}(\cdot)$ denotes taking the maximum value, while in DCO-OFDM $\varepsilon_{\mathsf{top}}^{(\mathsf{DCO})} = V_{\mathsf{max}} - B_{\mathsf{DC}}$ and $\varepsilon_{\mathsf{bottom}}^{(\mathsf{DCO})} = V_{\mathsf{min}} - B_{\mathsf{DC}}$.

In ACO-OFDM, the iterative symbol clipping times of the symbol $\boldsymbol{x}_{\mathsf{IFFT}}$ can be derived from the maximum amplitude value of the subcarrier signal, the top clipping levels and the number of LEDs, which can be calculated by:

$$\mu_{\mathsf{ACO}} = \mathsf{min}\Big(\mathsf{max}\Big(\Big\lceil \frac{\mathsf{max}(\boldsymbol{x}_{\mathsf{IFFT}}^{(1)}(i))}{\varepsilon_{\mathsf{top}}} \Big\rceil\Big), K\Big), \tag{7}$$

where $i = 1, 2, \cdots, N$, $\mathsf{min}(\cdot)$ denotes taking the minimum value, $\lceil \cdot \rceil$ denotes integer ceiling function. In DCO-OFDM, the iterative symbol clipping times of the symbol $\boldsymbol{x}_{\mathsf{IFFT}}$ can be calculated as:

$$\mu_{\mathsf{DCO}} = \mathsf{min}\Big(\mathsf{max}\Big(\Big\lceil \frac{\mathsf{max}(\boldsymbol{x}_{\mathsf{IFFT}}^{(1)}(i))}{\varepsilon_{\mathsf{top}}} \Big\rceil, \Big\lceil \frac{\mathsf{min}(\boldsymbol{x}_{\mathsf{IFFT}}^{(1)}(i))}{\varepsilon_{\mathsf{bottom}}} \Big\rceil\Big), K\Big), \tag{8}$$

Symbol $\boldsymbol{x}_{\mathsf{IFFT}}^{(1)}$ whose amplitude lies within $[K\varepsilon_{\mathsf{bottom}}, K\varepsilon_{\mathsf{top}}]$ can be transmitted completely without clipping distortion. However, if the amplitude of $\boldsymbol{x}_{\mathsf{IFFT}}^{(1)}$ goes beyond $[K\varepsilon_{\mathsf{bottom}}, K\varepsilon_{\mathsf{top}}]$, this means that it is subject to clipping distortion during transmission. Only if the total number of LEDs is large enough that the symbol, $\boldsymbol{x}_{\mathsf{IFFT}}^{(1)}$, can be fully transmitted without clipping distortion. Following the Bussgang theorem and the central limit theorem (CLT) [17], the nonlinear distortion is modeled as an attenuation of the received information-carrying subcarriers plus a zero-mean complex-valued non-Gaussian clipping noise. After adaptive iterative symbol clipping, the O-OFDM symbol can be expressed as:

$$\boldsymbol{x}_{\mathsf{clip}} = \boldsymbol{x}_{\mathsf{clip}}^{(1)} + \boldsymbol{x}_{\mathsf{clip}}^{(2)} + \cdots + \boldsymbol{x}_{\mathsf{clip}}^{(k)} = \eta \boldsymbol{x}_{\mathsf{IFFT}} + \boldsymbol{n}_{\mathsf{clip}}, \tag{9}$$

where $\boldsymbol{n}_{\mathsf{clip}}$ is the zero-mean non-Gaussian clipping noise, η is attenuation factor and can be derived as follows:

$$\eta = Q(K\lambda_{\mathsf{bottom}}) - Q(K\lambda_{\mathsf{top}}), \tag{10}$$

where, $Q(\cdot)$ is the complementary cumulative distribution function, λ_{top} and $\lambda_{\mathsf{bottom}}$ are the normalized top and bottom clipping levels, which can be expressed respectively as: $\lambda_{\mathsf{top}} = \varepsilon_{\mathsf{top}}/\sigma_0$ and $\lambda_{\mathsf{bottom}} = \varepsilon_{\mathsf{bottom}}/\sigma_0$.

Next, creating cyclic prefix (CP) extensions and appending respectively to the beginning of these symbols $\boldsymbol{x}_{\mathsf{clip}}^{(1)}, \boldsymbol{x}_{\mathsf{clip}}^{(2)}, \cdots, \boldsymbol{x}_{\mathsf{clip}}^{(k)}$ to mitigate ISI and inter-carrier interference (ICI). Then, these trains of symbols with CP are subjected to a digital-to-analog (D/A) converter and the DC bias are added to obtain the signal that drives the LED lighting, which are $\boldsymbol{x}_{\mathsf{LED}}^{(1)}, \boldsymbol{x}_{\mathsf{LED}}^{(2)}, \cdots, \boldsymbol{x}_{\mathsf{LED}}^{(k)}$, where the k-th drive signal can be expressed as:

$$\boldsymbol{x}_{\mathsf{LED}}^{(k)} = \boldsymbol{x}_{\mathsf{clip}}^{(k)} + B_{\mathsf{DC}}. \tag{11}$$

Finally, these drive signals are transmitted simultaneously to the LEDs, i.e. the k-th signal is transmitted to the k-th LED. Note that LEDs are set close to each other and placed to emit light in the same direction, i.e., same azimuth and elevation angles, the attenuation of the channel paths are very similar, so the resulting channel paths are almost identical[13].

The optical power of the transmitted signal can be expressed as:

$$\begin{aligned} P_{\mathsf{opt}} =& \sigma_0(k\lambda_{\mathsf{top}}Q(k\lambda_{\mathsf{top}}) + k\lambda_{\mathsf{bottom}}(1 - Q(k\lambda_{\mathsf{bottom}})) \\ &+ \varphi(k\lambda_{\mathsf{bottom}}) - \varphi(k\lambda_{\mathsf{top}})) + kB_{\mathsf{DC}}, \end{aligned} \tag{12}$$

where $\varphi(\cdot)$ represents the probability density function (PDF) of a standard normal distribution.

The transmission speed of information is measured by analyzing the bit rate. The bit rate can be calculated by:

$$R_{\mathsf{b}} = \frac{\zeta W \log_2(M)}{2}, \tag{13}$$

where W is the modulation bandwidth of the O-OFDM symbols.

2.2 Receiver

Optical signals are transmitted over an optical wireless channel and their transmission intensity is detected at the receiver by a photodiode(PD), and signals are distorted by the additive white Gaussian noise (AWGN). Following from that, the analogue signal is converted into a digital signal by means of an analogue-to-digital (A/D) conversion block. The received signal before A/D is given by

$$\boldsymbol{y} = \gamma(\boldsymbol{x}_{\mathsf{LED}}^{(1)} + \boldsymbol{x}_{\mathsf{LED}}^{(2)} + \cdots + \boldsymbol{x}_{\mathsf{LED}}^{(k)}) + \boldsymbol{w}, \tag{14}$$

where γ is the optical-to-electrical conversion factor, and $\boldsymbol{w}$ is AWGN, which represents the sum of the receiver thermal noise and shot noise due to background light, and its single-sided power spectral density is N_0.

It is followed by a serial-to-parallel (S/P) conversion and the removal of the CP extension for the decomposed symbols. Next, the CP-removed symbols are transferred to the fast Fourier transformation (FFT) block to obtain the frequency domain signal. This frequency domain signal can be expressed as follows:

$$\boldsymbol{Y}_{\mathsf{FFT}} = \alpha\gamma\eta\boldsymbol{X}_{\mathsf{mapping}} + \gamma k\boldsymbol{B} + \gamma\boldsymbol{N}_{\mathsf{clip}} + k\boldsymbol{W}_{\mathsf{AWGN}}, \tag{15}$$

where $\boldsymbol{W}_{\mathsf{AWGN}}$ is the AWGN in the frequency domain, $\boldsymbol{B}$ is the DC bias in the frequency domain and $\boldsymbol{B} = [\sqrt{N}B_{\mathsf{DC}}, 0, 0, \cdots, 0]^{\mathsf{T}}$, and $\boldsymbol{N}_{\mathsf{clip}}$ is the clipping noise in the frequency domain. In accordance with the CLT, the clipping noise can be modeled as a Gaussian process. Utilizing the statistics of truncated Gaussian distribution, the variance of the clipping noise can be expressed respectively in ACO-OFDM and DCO-OFDM as follows:

$$\begin{aligned}\sigma^2_{\mathsf{clip,ACO}} =& \frac{P_{\mathsf{s(elec)}}}{2}\{\eta(K^2\lambda^2_{\mathsf{bottom}}+1) - 2\eta^2 - K\lambda_{\mathsf{bottom}}[\varphi(K\lambda_{\mathsf{bottom}}) \\ &- \varphi(K\lambda_{\mathsf{top}})] - \varphi(K\lambda_{\mathsf{top}})(K\lambda_{\mathsf{top}} - K\lambda_{\mathsf{bottom}}) + Q(K\lambda_{\mathsf{top}} \\ &- K\lambda_{\mathsf{bottom}})^2\},\end{aligned} \tag{16}$$

$$\begin{aligned}\sigma^2_{\mathsf{clip,DCO}} =& P_{\mathsf{s(elec)}}\{\eta - \eta^2 - \{\varphi(K\lambda_{\mathsf{bottom}}) - \varphi(K\lambda_{\mathsf{top}}) + [1 \\ &- Q(K\lambda_{\mathsf{bottom}})]K\lambda_{\mathsf{bottom}} + Q(K\lambda_{\mathsf{top}})K\lambda_{\mathsf{top}}\}^2 + [1 \\ &- Q(K\lambda_{\mathsf{bottom}})]K^2\lambda^2_{\mathsf{bottom}} + Q(K\lambda_{\mathsf{top}})K^2\lambda^2_{\mathsf{top}} \\ &+ \varphi(K\lambda_{\mathsf{bottom}})K\lambda_{\mathsf{bottom}} - \varphi(K\lambda_{\mathsf{top}})K\lambda_{\mathsf{top}}\}.\end{aligned} \tag{17}$$

To counter channel effects, the frequency domain O-OFDM symbol $\boldsymbol{Y}_{\mathsf{FFT}}$ is equalized in the equalization block. In the next step, the frame structure of the mapped symbol at the transmitter makes it easy for the receiver to determine which subcarriers carry valid information in each O-OFDM symbol.

Finally, the extracted symbols are demodulated by using a maximum likelihood M-QAM detector, and the bit error rate (BER) of any M-QAM constellation can be calculated as follow:

$$P_{\mathsf{e}} = \frac{4(\sqrt{M}-1}{\mathsf{log}_2(M)\sqrt{M}}Q\left(\sqrt{\frac{3\mathsf{log}_2(M)}{M-1}\Gamma_{\mathsf{SNR}}}\right), \tag{18}$$

where Γ_{SNR} is the effective signal-to-noise ratio(SNR), which can be calculated as follows:

$$\Gamma_{\mathsf{SNR}} = \frac{\alpha^2\eta^2\gamma^2 P_{\mathsf{s,elec}}}{\mathsf{log}_2(M)(\sigma^2_{\mathsf{clip}} + kWN_{\mathsf{o}})}. \tag{19}$$

3 Performance Analysis

In the following, a simulation model of an O-OFDM system applying the AISC scheme is built by using MATLAB and its performance is also analyzed using

the Monte Carlo methods. In addition, it is compared with the O-OFDM system using the traditional ISC scheme and the ASDST scheme. OSRAM white LEDs with the model number OSRAM LUW W5SM are considered in this paper. Some parameters considered in the simulation are shown in Table 1. The clipping levels can be calculated according to the data in Table 1. The top and bottom clipping levels in ACO-OFDM are $\varepsilon_{\mathsf{top}}^{(\mathsf{ACO})} = 0.8\text{V}$ and $\varepsilon_{\mathsf{bottom}}^{(\mathsf{ACO})} = 0\text{V}$ respectively, and the top and bottom clipping levels in DCO-OFDM are $\varepsilon_{\mathsf{top}}^{(\mathsf{DCO})} = 0.8\text{V}$ and $\varepsilon_{\mathsf{bottom}}^{(\mathsf{DCO})} = -0.1\text{V}$ respectively. Because the IFFT output signal and AWGN subject to Gaussian distribution, the Monte Carlo method is used to obtain the clipping times, BER, EVM, optical power, and bit rate.

Table 1 The parameters of the O-OFDM system applying the AISC scheme

symbol	value	Parameter
The number of OFDM symbols	N_{sym}	10000
the number of cyclic prefixes	N_{CP}	16
Turn-on voltage(V)	V_{min}	0.1
Maximum permissible voltage(V)	V_{max}	1
DC bias current(V)	B_{DC}	0.2
Power spectral density of the AWGN(dBm)	N_0	-10
Modulation bandwidth(MHz)	W	20
Optical-to-electrical conversion factor(A/W)	γ	1

3.1 The Clipping Times

Fig. 3 and Fig. 4 respectively show the clipping times in the ACO-OFDM and DCO-OFDM systems with 8 LEDs, where the X-axis represents the variance of the O-OFDM symbols, which varies from -10 dBm to 50 dBm, and the Y-axis represents the clipping times of the O-OFDM symbols.

Firstly, we can find from these two figures that the theoretical and simulation curves of the clipping times match perfectly, which demonstrates the correctness of the theoretical analysis of the clipping times. Secondly, the clipping times of the AISC scheme and the conventional ISC scheme were compared. In the AISC scheme, it can be found that $\mu = 1$ when σ_0^2 is small. And μ keeps increasing as σ_0^2 continues to increase, until $\mu = 8$. (For example, in the case of $N = 256$, $\mu = 8$ when $\sigma_0^2 = 38\text{dBm}$ in ACO-OFDM). Because the clipping times of O-OFDM symbols in the AISC scheme need to be determined according to the signal amplitude, the clipping times of the AISC scheme are less than the traditional ISC scheme when σ_0^2 is small. μ does not increase as σ_0^2 when $\mu = 8$. Finally, the O-OFDM systems applying the AISC scheme with different subcarrier numbers are compared. This illustrates that as the number of subcarriers increases, it requires more clipping times. For example, in

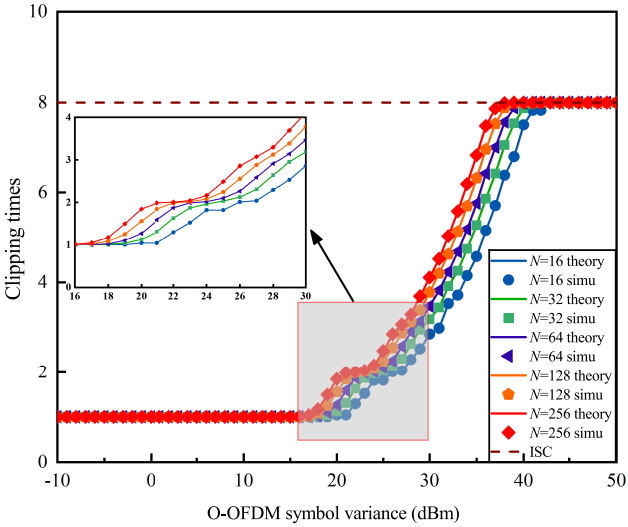

Fig. 3 The clipping times of ACO-OFDM system

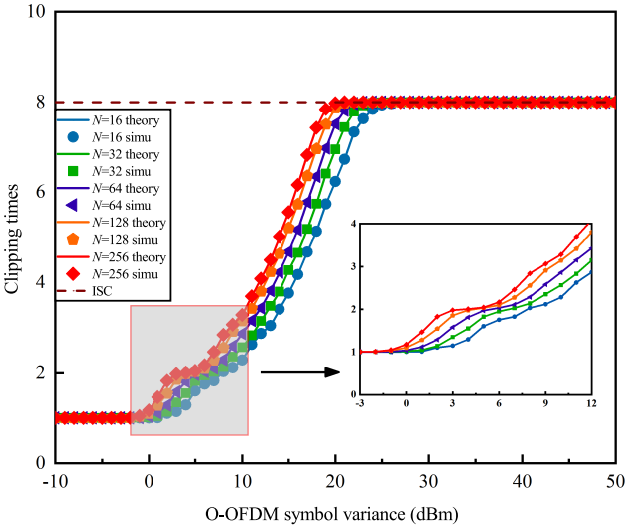

Fig. 4 The clipping times of DCO-OFDM system

ACO-OFDM, when the symbol variance is from 16dBm to 43dBm, the clipping times is consistently greater for a large number of subcarriers than for a small number of subcarriers.

3.2 The BER

The theoretical analysis and simulation results of DCO-OFDM and ACO-OFDM systems with different number of LEDs applying AISC scheme are

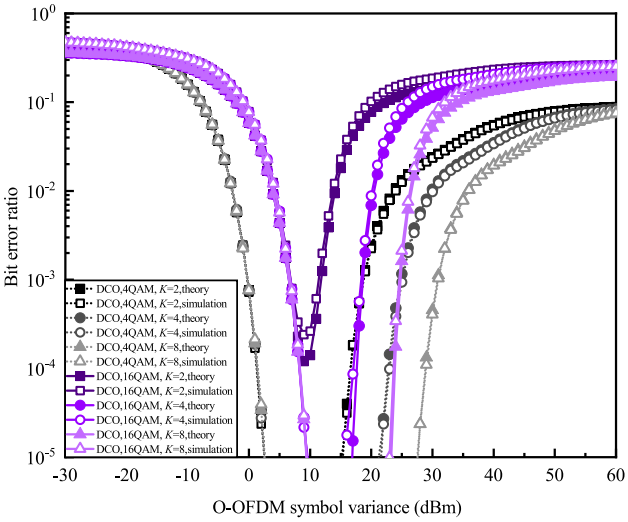

Fig. 5 BER performance with different number of LEDs for DCO-OFDM system

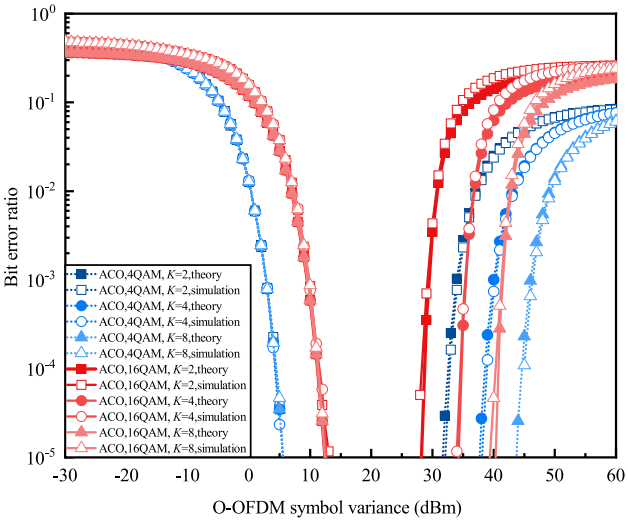

Fig. 6 BER performance with different number of LEDs for ACO-OFDM system

shown respectively in Fig. 5 and Fig. 6. Firstly, it can be observed that the theoretical and the simulation BER curves match perfectly, which verifies the correctness of the theoretical analysis of BER. Secondly, it can be noticed that the BER performance of 4QAM modulation is significantly better than that of 16QAM. Finally, it can be found that the BER performance curves for K=2, K=4 and K=8 exactly coincide at low variance of the O-OFDM symbols. This is because σ_0^2 is small (i.e., the amplitude of the O-OFDM symbols is within $[K\varepsilon_{\mathsf{bottom}}, K\varepsilon_{\mathsf{top}}]$), the required clipping times is less than K, and it does

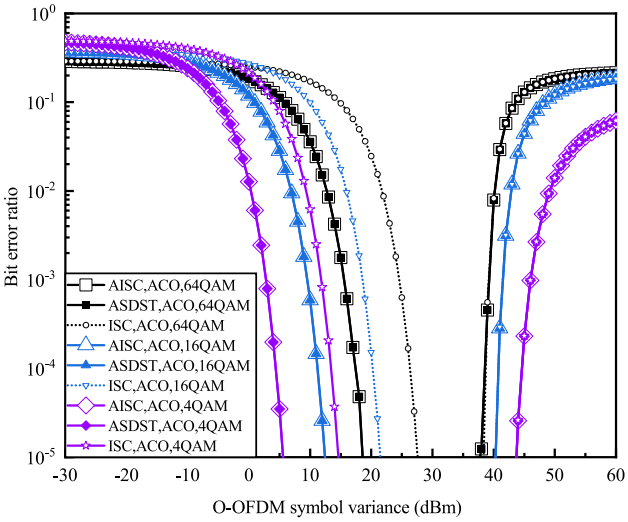

Fig. 7 BER performance comparison of AISC scheme, ASDST scheme and ISC scheme in ACO-OFDM

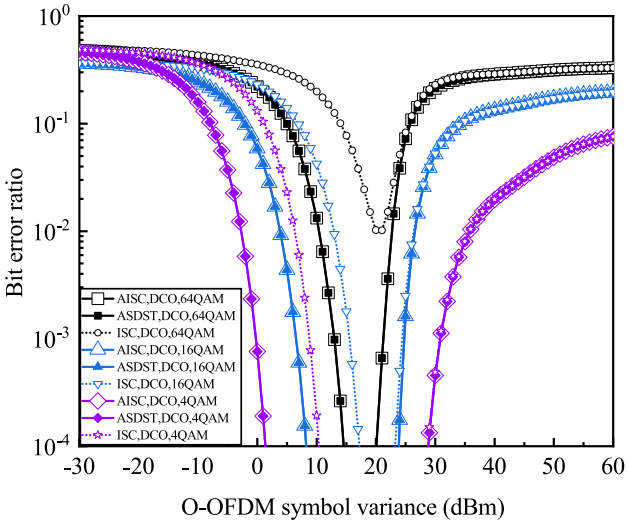

Fig. 8 BER performance comparison of AISC scheme, ASDST scheme and ISC scheme in DCO-OFDM

not generate clipping noise, so the BER does not vary with K. At higher O-OFDM symbol variance, it can be found that the BER performance is better as K becomes higher. This is because when K is larger, more OFDM symbols can be transmitted without distortion, meanwhile OFDM symbols with larger variance generate less clipping noise during transmission. For example, in the case of $\sigma_0^2 = 44$dBm and 4QAM, the BER of K=8 is about 2.5×10^{-5}, the BER

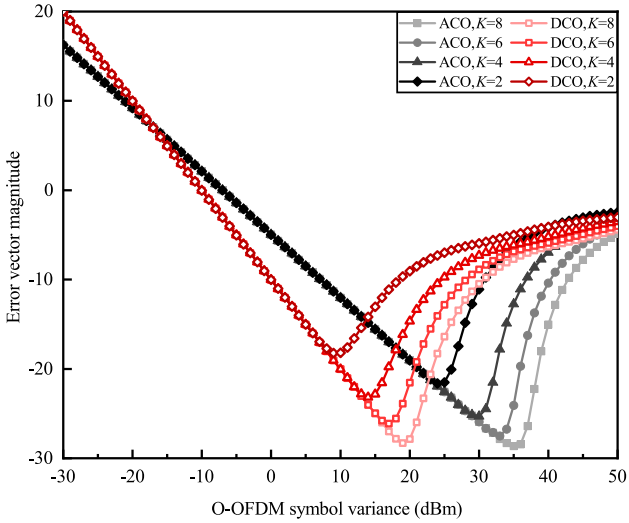

Fig. 9 EVM performance comparison in 4QAM modulation

of K=4 is about 1.4×10^{-2}, and the BER of K=2 is about 4.5×10^{-2} in ACO-OFDM. However, as the O-OFDM symbol variance continues to increase, the BER performance degrades significantly. This is because the amplitude of O-OFDM symbols will exceed $[K\varepsilon_{\text{bottom}}, K\varepsilon_{\text{top}}]$, resulting in the appearance of clipping noise, and the clipping noise will also increase as σ_0^2 increases.

The BER performance of ACO-OFDM and DCO-OFDM systems applying the ISC scheme , ASDST scheme and the AISC scheme with different QAM modulation orders and K=8 are compared in Fig. 7 and Fig. 8. Firstly, it can be found that the BER performance curves of the AISC scheme and the ASDST scheme at different QAM modulation orders are exactly coincident, which illustrates that these two schemes have the same BER performance in ACO-OFDM and DCO-OFDM systems. Next, the BER performance of AISC scheme is significantly better than that of ISC scheme for ACO-OFDM and DCO-OFDM systems with different QAM modulation orders when σ_0^2 is small. Which proves that the proposed AISC scheme can significantly improve the BER performance. In the ISC scheme, O-OFDM symbols with small variance generate multiple all-zero symbols due to a fixed clipping times. Therefore, the AWGN noise increases when the symbols are combined at the receiver side, which makes the BER decrease. However, the AISC scheme eliminates the all-zero symbols, so the BER is improved.

3.3 The EVM

The EVM[18] performance is compared in Fig. 9 for different number of LEDs. In ACO-OFDM, when σ_0^2 is small, the EVM performance curves with different number of LEDs are completely matched. This is because when $\mu < K$, OFDM symbols will not generate clipping noise during transmission. When the OFDM

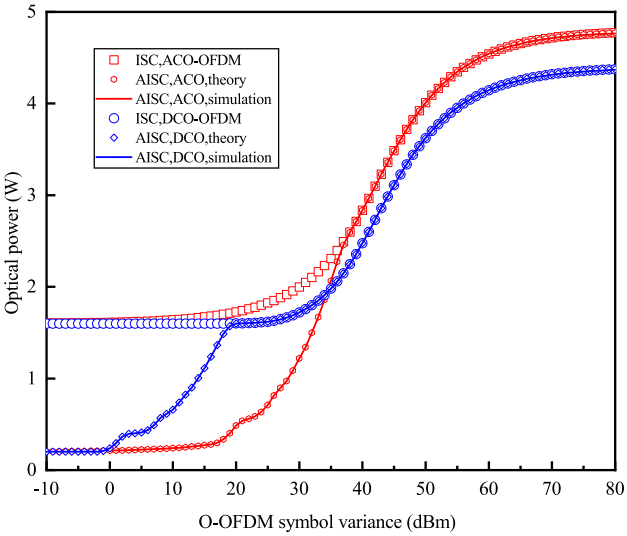

Fig. 10 The optical power for AISC scheme and ISC scheme

symbol variance is large, the EVM performance starts to degrade. For example, when $\sigma_0^2 = 24$dBm , it can be found that the EVM performance of K=2 starts to degrade. This is because the OFDM symbols require clipping times starting to be greater than 2 at this point, which causes the generation of clipping noise. Moreover, the clipping noise becomes larger as clipping times continues to increase. In addition, the EVM performance of K=4, K=6 and K=8 starts to decrease at $\sigma_0^2 = 29$dBm , $\sigma_0^2 = 32$dBm and $\sigma_0^2 = 36$dBm, respectively.

3.4 The Optical Power

The theoretical analysis and simulation curves of the optical power in the ACO-OFDM and DCO-OFDM systems applying the AISC scheme and ISC scheme are shown in Fig. 10.

When σ_0^2 is small, the optical power of the AISC scheme is significantly reduced compared to the ISC scheme. This is because in the ISC scheme, the all-zero symbols that appear consume optical power after adding the DC bias. However, the AISC scheme eliminates the all-zero symbol using the adaptive method to avoid the consumption of optical power, thereby improving the optical power efficiency. It proves that the scheme proposed in this paper has obvious advantages in saving optical power.

3.5 The Bit Rate

The bit rate curves of ISC scheme, AISC scheme and ASDST scheme with different QAM modulation orders and $K = 4$ are shown respectively in Fig.11 and Fig.12. It can be observed that the bit rates of the ISC scheme and the AISC scheme are exactly equal. This is because the OFDM symbols generated

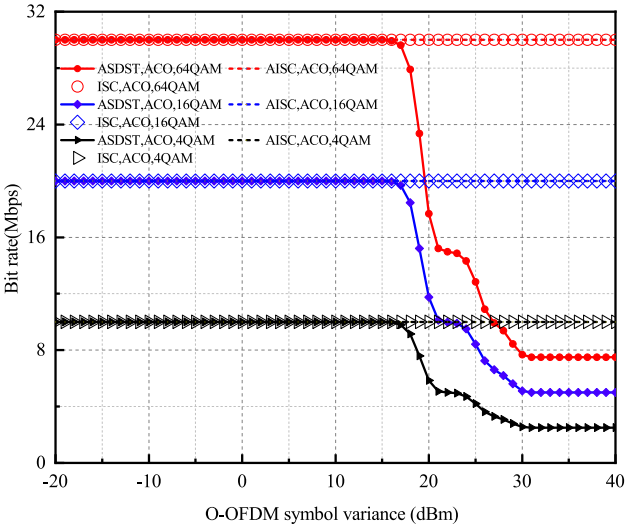

Fig. 11 The bit rate of ACO-OFDM systems applying different schemes

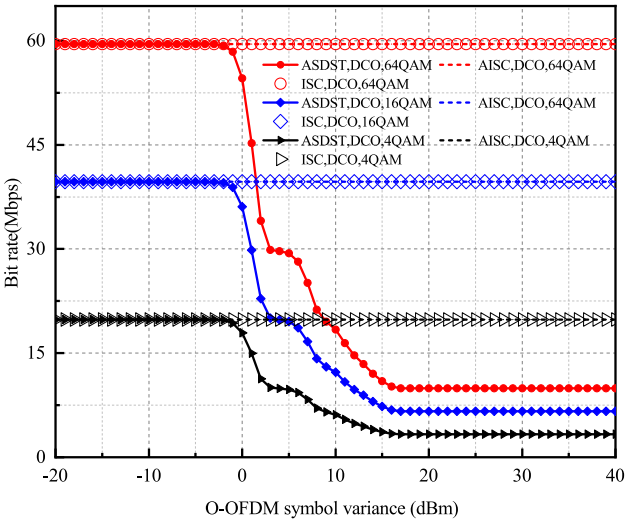

Fig. 12 The bit rate of DCO-OFDM systems applying different schemes

in the AISC and ISC schemes are transmitted in parallel through multiple LEDs simultaneously. Also the bit rate does not vary with the symbol variance. When σ_0^2 is small, because the clipping times of the ASDST scheme is 1, the bit rates of the ASDST scheme, the AISC scheme and the ISC scheme are completely equal. The clipping times of the ASDST scheme is constantly increasing as σ_0^2 becomes larger, resulting in a decreasing bit rate. The clipping times of the ASDST scheme reaches 4 when $\sigma_0^2 \geq 31$dBm, it can be found that the bit rate of the ASDST scheme starts not varying with the O-OFDM

symbol variance. By comparing Fig.11 and Fig.12, it can be found that ACO-OFDM and DCO-OFDM have similar trends, and it can also be found that the bit rate of ACO-OFDM is one-half of that of DCO-OFDM. The simulation results show that the proposed scheme is effective in increasing the system transmission rate compared to the ASDST scheme.

4 Conclusion

For the OFDM-based visible light communication system, the adaptive O-OFDM iterative symbol clipping scheme is proposed to effectively mitigate the nonlinear distortion caused by the high PAPR characteristics of O-OFDM symbols and the nonlinear characteristics of LEDs. Without reducing the bit rate of the conventional ISC scheme, this scheme exploits the adaptive mechanism to effectively reduce the clipping times and eliminate all-zero symbols when the variance of O-OFDM symbols is lower, and it also improves the efficiency of optical power and enhances the BER performance.

Data Availability Statement

The datasets analysed during the current study are available from the corresponding author on reasonable request.

Declarations

Conflicts of Interest The authors declare they have no financial interests.
Code Availability The code will made be available on reasonable request.

References

[1] Tsonev, D. , Chun, H. , Rajbhandari, S. , Mckendry, J. , & O'Brien, D. . (2014). A 3-gb/s single-led ofdm-based wireless vlc link using a gallium nitride μLED. IEEE Photonics Technology Letters, 26(7), 637-640.

[2] Tsonev, D., & Haas, H. (2014, June). Avoiding spectral efficiency loss in unipolar OFDM for optical wireless communication. In 2014 IEEE international conference on communications (ICC) (pp. 3336-3341). IEEE.

[3] Mesleh, R., Elgala, H., & Haas, H. (2011). On the performance of different OFDM based optical wireless communication systems. Journal of Optical Communications and Networking, 3(8), 620-628.

[4] Armstrong, J., & Schmidt, B. J. (2008). Comparison of asymmetrically clipped optical OFDM and DC-biased optical OFDM in AWGN. IEEE Communications Letters, 12(5), 343-345.

[5] Sheu, J. S., Li, B. J., & Lain, J. K. (2017). LED non-linearity mitigation techniques for optical OFDM-based visible light communications. IET Optoelectronics, 11(6), 259-264.

[6] Elgala, H., Mesleh, R., & Haas, H. (2009). Non-linearity effects and predistortion in optical OFDM wireless transmission using LEDs. International Journal of Ultra Wideband Communications and Systems, 1(2), 143-150.

[7] Asatani, K., & Kimura, T. (1978). Linearization of LED nonlinearity by predistortions. IEEE Journal of Solid-State Circuits, 13(1), 133-138.

[8] Stepniak, G., Siuzdak, J., & Zwierko, P. (2013). Compensation of a VLC phosphorescent white LED nonlinearity by means of Volterra DFE. IEEE Photonics Technology Letters, 25(16), 1597-1600.

[9] Qian, H., Yao, S. J., Cai, S. Z., & Zhou, T. (2014). Adaptive postdistortion for nonlinear LEDs in visible light communications. IEEE Photonics Journal, 6(4), 1-8.

[10] Liu, H., Jiang, Y., Zhu, X., & Wang, T. (2019, May). Low-complexity and robust PAPR reduction and LED nonlinearity mitigation for UACO-OFDM LiFi systems. In ICC 2019-2019 IEEE International Conference on Communications (ICC) (pp. 1-6). IEEE.

[11] Ying, K., Yu, Z., Baxley, R. J., Qian, H., Chang, G. K., & Zhou, G. T. (2015). Nonlinear distortion mitigation in visible light communications. IEEE Wireless Communications, 22(2), 36-45.

[12] Ankarali, Z. E., Hussain, S. I., Abdallah, M., Qaraqe, K., Arslan, H., & Haas, H. (2014, September). Clipping noise mitigation using partial transmit sequence for optical OFDM systems. In 2014 3rd International Workshop in Optical Wireless Communications (IWOW) (pp. 80-84). IEEE.

[13] Mesleh, R. (2013). LED clipping distortion compensation in optical wireless communication via multiple transmit LEDs. Photonic Network Communications, 26(1), 25-31.

[14] Mesleh, R., Elgala, H., & Haas, H. (2012). LED nonlinearity mitigation techniques in optical wireless OFDM communication systems. Journal of Optical Communications and Networking, 4(11), 865-875.

[15] Jia, K., Yang, B., Cao, M., Lin, Y., Li, S., & Hao, L. (2020). An Adaptive Symbol Decomposition With Serial Transmission for O-OFDM-Based VLC System. IEEE Communications Letters, 25(3), 916-920.

[16] Wang, J., Xu, Y., Ling, X., Zhang, R., Ding, Z., & Zhao, C. (2016). PAPR analysis for OFDM visible light communication. Optics express, 24(24), 27457-27474.

[17] Zhang, X., Liu, P., Liu, J., & Liu, S. (2015, December). A DCO-OFDM system employing beneficial clipping method. In 2015 ITU Kaleidoscope: Trust in the Information Society (K-2015) (pp. 1-6). IEEE.

[18] Elgala, H., Mesleh, R., & Haas, H. (2009, April). A study of LED nonlinearity effects on optical wireless transmission using OFDM. In 2009 IFIP International Conference on Wireless and Optical Communications Networks (pp. 1-5). IEEE.

Kejun Jia received his M.S. degree in communication and information system from Xi'an University of Technology, Xi'an, P. R. China and Ph.D. degree in communication and information system from Southwest Jiaotong University, Chengdu, P. R. China in 2007 and 2018, respectively. Since 2001, he has been in the School of Computer and Communication, Lanzhou University of Technology, Lanzhou, P. R. China, where he is currently a professor. His research interests include indoor visible light communications, multi-carrier systems as well as the next-generation wireless communications.

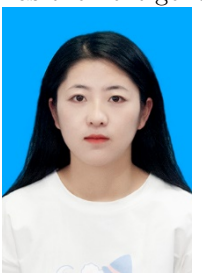

Cuicui Qin received the B.E. degree in network engineering from Lanzhou Technology and Business College, Lanzhou, China, in 2019. She is currently working toward the M.E. degree at Lanzhou University of Technology, Lanzhou, China. Her research interest is in visible light communication.

Boran Yang received the B.E. degree in communication engineering and the M.E. degree in communication and information system from Lanzhou University of Technology, Lanzhou, China, in 2018 and 2021, respectively. He is currently working toward the Ph.D. degree at the Southwest Jiaotong University, Chengdu, China. His research interests include visible light communication and massive machine-type communication.

Minghua Cao received his BEng degree in communication engineering from Gansu University of Technology, Lanzhou, China, in 2002, his MEng degree in signal and information processing from Lanzhou University of Technology, Lanzhou, China, in 2009, and his PhD in electronic science and technology from Beijing University of Posts and Telecommunications, Beijing, China, in 2016. He is currently an associate professor with the School of Computer and Communication, Lanzhou University of Technology. His research interests include free space optical communication systems and low-cost radio-over-fiber networks.

Suoping Li, IEEE Member, is a full professor of school of science at Lanzhou University of Technology (LUT), China. He received the Ph.D. degree in Signal and Information Processing from Beijing Jiaotong University, China, in 2004. He also hold a M.Sc. degree in Stochastic Model with Applications from Lanzhou University in 1996, and B.Sc. degree in Mathematics from Northwest Normal University in 1986. He was a visiting scholar at Swiss Federal Institute of Technology Zurich (ETH) from May 2007 to May 2008, and also a visiting professor at American East Texas Baptist University (ETBU) from Aug to Dec 2011. He completed short academic visits at Universite de Technologie Belfort-Montbeliard (UTBM) France in 2017 and at Università degli Studi dell'Aquila (UNIVAQ) Italy in 2018. His primary research interests include optimization and control of stochastic system, analysis of random signal, modeling analysis of wireless communication network, analysis and design of data communications protocol.